electronics

MDPI

Article

Fixed-Time Bearing-Only Formation Control Without a Global Coordinate Frame

Hanqiao Huang [1,2], Mengwen Lu [2], Bo Zhang [1,3,*] and Qian Wang [4]

[1] Research Center for Unmanned System Strategy Development, Northwestern Polytechnical University, Xi'an 710072, China; huanghanqiao@nwpu.edu.cn
[2] Unmanned System Research Institute, Northwestern Polytechnical University, Xi'an 710072, China; lumw@mail.nwpu.edu.cn
[3] Research & Development Institute of Northwestern Polytechnical University in Shenzhen, Shenzhen 518057, China
[4] National Elite Institute of Engineering, Northwestern Polytechnical University, Xi'an 710072, China; qianwang@nwpu.edu.cn
* Correspondence: zhbo@nwpu.edu.cn

Abstract

This work addresses distributed fixed-time bearing-only formation stabilization for multi-agent systems lacking shared orientation knowledge. Addressing the challenge of missing global coordinate alignment in multi-agent systems, this work introduces a novel distributed estimator ensuring almost globally fixed-time convergence of orientation estimates. Leveraging this estimator, we develop a distributed bearing-only formation control law specifically designed for agents governed by double-integrator dynamics, guaranteeing fixed-time convergence. Comprehensive stability analysis proves the almost global fixed-time stability of the overall closed-loop system. Crucially, the proposed control strategy drives actual formation to achieve the desired geometric pattern with almost global exponential convergence within a fixed time bound. Rigorous numerical experiments corroborate the theoretical framework.

Keywords: bearing-only formation; distributed fixed-time control; free of global coordinate frame; bearing rigidity

check for updates

Academic Editor: Sung Jin Yoo

Received: 4 June 2025
Revised: 14 July 2025
Accepted: 23 July 2025
Published: 29 July 2025

Citation: Huang, H.; Lu, M.; Zhang, B.; Wang, Q. Fixed-Time Bearing-Only Formation Control Without a Global Coordinate Frame. *Electronics* **2025**, *14*, 3021. https://doi.org/10.3390/electronics14153021

Copyright: © 2025 by the authors. Licensee MDPI, Basel, Switzerland. This article is an open access article distributed under the terms and conditions of the Creative Commons Attribution (CC BY) license (https://creativecommons.org/licenses/by/4.0/).

1. Introduction

Distributed coordination of multi-agent networks for formation tasks has seen significant research interest [1,2]. These systems achieve target geometries through kinematic constraints between neighboring agents, with control strategies classified by sensed variables: displacement, distance, or bearing [2]. Previous studies have conducted a series of investigations on formation control based on distance constraints. Rigidity maintenance in n-dimensional undirected formations is topologically guaranteed by gradient-based controllers, as proven in [3] through local asymptotic stability analysis, showing that infinitesimal rigidity is not required for single-integrator agents and leveraging topological equivalence to extend the result to double-integrator agents. Ref. [4] proposed a modified distributed gradient control law achieving finite-time stabilization of distance-constrained rigid formation shapes in any dimension. However, compared to distance-constrained approaches, formation control based on bearing information has been relatively less studied. Furthermore, the principles of distributed multi-agent formation control can be further applied to the domain of spacecraft formation flying, enabling robust and autonomous

coordination for complex on-orbit missions such as cooperative observation missions [5,6] and formation maintenance in highly dynamic orbits [7]. This study investigates a distributed formation control problem based on bearing measurements, in which agents collaboratively achieve a desired geometric configuration without centralized coordination. Unlike approaches relying on relative position or distance measurements in [2], the bearing-based approach operates through neighbor-relative bearing observations, without the need for relative distance or position information. This dramatically slashes sensing overhead while facilitating real-time executable formation control on embedded sensing platforms. For resource-limited multi-agent systems, bearing data acquisition via vision-based sensors [8] or distributed RF arrays [9,10] offers implementation advantages.

It is worth emphasizing that bearing-related measurements may be expressed either in the form of a unit direction vector or through the relative angle between two such vectors [11,12], and recent work considered communication delay and switching topology on bearing-based control [13]. Consequently, bearing-based formation control problems are typically tackled using two main strategies. One common strategy involves regulating inter-agent bearing angles, which has been extensively examined in earlier works focusing on formations composed of three or four agents, such as [14,15]. Extensions of this method to n -agent systems have been explored in works such as [16,17]. However, the bearing angle approach faces significant challenges when applied to formation control in three-dimensional spaces, limiting its scalability and applicability in such scenarios. The second approach to bearing-based formation control leverages bearing rigidity theory in $\mathbb{R}^d$ [18–21]. For planar formations with undirected sensing topologies, a distributed control strategy was introduced in [22], aiming to drive the formation toward a target geometric configuration. Furthermore, the approach proposed in [20] ensures that any framework exhibiting infinitesimal bearing rigidity can be stabilized with almost global exponential convergence, using only bearing information. For directed formations, refs. [23,24] have focused on specific structures such as leader-first follower formations in $\mathbb{R}^d$ and directed cycle formations in $\mathbb{R}^2$, demonstrating the applicability of bearing rigidity theory to various directed sensing scenarios.

However, existing bearing-based methods predominantly assume global reference frames. Nonetheless, in certain scenarios, agents may not have access to global reference frames, which poses additional challenges for coordination and control in distributed systems. When agents lack shared directional reference, $SE(3)$ bearing rigidity enables distributed 3D formation control through relative orientation measurements [25]. While $SO(3)$ alignment strategies coordinate agent attitudes and bearings [26,27], their effectiveness is limited by stringent initial orientation requirements. Recent advances in $SO(3)$ synchronization include finite-time solutions for leader–follower [28] and multi-agent systems [29]. It is essential to note that finite-time control bounds convergence time in terms of initial states, whereas fixed-time control enforces a uniform convergence within a predetermined time horizon T_{max}, which remains independent of the initial conditions; this uniformity is critical for global reference-free systems with potentially dispersed agents. Ref. [30] proposed a fixed-time synchronized control framework, achieving simultaneous convergence of multiple state variables within a fixed time for the first time, and resolving the singularity issue in traditional fixed-time control via a norm-normalized sign function design. To overcome alignment limitations, estimation-based methods [31] reconstruct orientations from vector-space auxiliary variables, achieving almost-global convergence without initial constraints. Moreover, this estimation approach is applicable to systems in arbitrary dimensions, offering greater flexibility in addressing formation control tasks.

This study addresses the fixed-time stabilization of multi-agent formations through the adjustment of relative bearing angles among neighboring agents, all without a global

coordinate frame. Specifically, the challenge lies in achieving formation control using only bearing measurements, without access to a common global reference frame, while ensuring guaranteed convergence within a predefined time and robustness against model uncertainties and external disturbances. In comparison with controllers that guarantee only asymptotic stability and finite-time controllers proposed in [32], fixed-time controllers offer several advantages, including faster convergence rates, better tolerance to external perturbations, and increased resilience against model uncertainties [33]. Unlike finite-time control that shares the above advantages, fixed-time algorithms possess the capability to ensure a convergence time bound that remains unaffected by the initial conditions [34]. Building upon the framework of fixed-time convergence theory, the works in [35,36] investigated consensus protocols for both integrator-type multi-agent systems and more complex dynamical models. Distinguished from prior research, this work investigates fixed-time formation control relying solely on bearing measurements in scenarios where the global coordinate frame is unavailable. Therefore, this work's fundamental theoretical contributions consist of the following:

1. First, a fixed-time orientation estimation law is developed, laying the groundwork for deeper and more comprehensive investigations.
2. Therefore, leveraging the proposed novel orientation observer scheme, a key contribution of this study is the development of a bearing-based formation controller that functions independently of any global reference frame. Comprehensive analyses are provided to demonstrate almost-global stability and ensure convergence within a fixed time for the proposed mechanisms.
3. Finally, a collision-free condition for the formation control is derived to avoid collision when only bearing information is available.

An overview of the paper's organization is provided below. Section 2 details mathematical preliminaries. Section 3 formulates the control problem and presents core innovations: a novel fixed-time orientation estimation law and a bearing-only formation controller. We conclude with Section 4, validating the results through simulations. Section 5 summarizes our contributions.

2. Preliminaries

2.1. Fixed-Time Stability

This work investigates the nonlinear dynamical system, as shown below:

$$\dot{x} = f(t, x), x(0) = x_0, \tag{1}$$

where $x \in \mathbb{R}^d$ denotes the state vector, and the function $f : \mathbb{R}_+ \times \mathbb{R}^d \to \mathbb{R}^d$ is assumed to be nonlinear. In the case where $f(t, x)$ exhibits discontinuities, system (1) is analyzed using the Filippov solution concept. For a real-valued function $\varphi(t)$, the upper right-hand Dini derivative at time t is expressed as follows:

$$D^*\varphi(t) = \lim_{h \to +0} \sup \frac{\varphi(t+h) - \varphi(t)}{h}. \tag{2}$$

Here, we suppose that the origin serves as an equilibrium point of system (1).

Definition 1 ([37]). *The origin of system (1) attains global finite-time stability if and only if it is globally asymptotically stable and, crucially, for any initial state $x_0 \in \mathbb{R}^d$, there exists a finite convergence time $T(x_0)$, i.e., a non-negative real-valued function dependent on the initial condition, such that the solution trajectory $x(t, x_0)$ not only converges to zero at time $T(x_0)$ but*

thereafter remains precisely and identically zero for all subsequent time instants beyond this critical settling moment.

Definition 2 ([34]). *The equilibrium at the origin of system (1) is termed globally fixed-time stable if it meets the conditions for global finite-time stability; moreover, if there exists a constant upper bound $T_{\max} > 0$, the settling time for any initial state $x_0 \in \mathbb{R}^d$ does not exceed this bound. That is, the convergence time $T(x_0)$, defined as a function from $\mathbb{R}^d$ to the non-negative reals, satisfies $T(x_0) \leq T_{\max}$ for all possible x_0.*

The following lemma is instrumental to both the development and analysis of control laws, ensuring fixed-time stability.

Lemma 1 ([38]). *Suppose there exists a continuous and radially unbound function V that maps from the d-dimensional real space to a set of non-negative real numbers (including zero), denoted as $V : \mathbb{R}^d \to \mathbb{R}_+ \cup \{0\}$, and this function satisfies the following condition:*

1. $V(x) = 0 \Leftrightarrow x = 0$;
2. *If the trajectory $x(t)$ of system (1) fulfills the condition $D^+V(x(t)) \leq -\kappa_1 V^{\eta_1}(x(t)) - \kappa_2 V^{\eta_2}(x(t))$, with constant $\kappa_1, \kappa_2 > 0$, $\mu_0 > 1$, $\eta_1 = 1 - (1/2\mu_0)$, and $\eta_2 = 1 + (1/2\mu_0)$. In this case, the equilibrium point at the origin of system (1) exhibits global fixed-time stability. Furthermore, the settling time is uniformly bounded by the following:*

$$T_{\max} = \frac{\pi\mu_0}{\sqrt{\kappa_1\kappa_2}}, \forall x_0 \in \mathbb{R}^d. \tag{3}$$

Lemma 2 ([35]). *Let $x_1, x_2, \ldots, x_n \geq 0$, $0 < u \leq 1$, and $v > 1$. Then,*

$$\begin{aligned} \sum_{i=1}^{n} x_i^u &\geq \left(\sum_{i=1}^{n} x_i\right)^u, \\ \sum_{i=1}^{n} x_i^v &\geq n^{1-v}\left(\sum_{i=1}^{n} x_i\right)^v. \end{aligned} \tag{4}$$

2.2. Graph Theory

Consider a directed graph $\mathcal{G} = (\mathcal{V}, \mathcal{E})$ comprising n vertices labeled $1, 2, \ldots, n$, where the directed edge set $\mathcal{E} \subset \mathcal{V} \times \mathcal{V}$ formally characterizes the unidirectional interconnection topology between distinct nodes. Each edge represents a directional link from one node to another. The edges are defined by ordered pairs $e_k = (i, j)$. Agent interactions adhere to a time-invariant digraph topology, with the geometric configuration $\mathcal{G}(q)$ embedded by assigning a position vector q_i to each node i. Agent i is said to have access to agent j's information whenever a directed edge (i, j) exists in $\mathcal{E}$. Its set of neighboring agents is represented as $\mathcal{N}_i \triangleq \{j \in \mathcal{V} : (i, j) \in \mathcal{E}\}$. For the purpose of this study, it is assumed that the communication between any two follower agents within this neighborhood is bidirectional.

2.3. Bearing Rigidity

The framework $\mathcal{G}_b(q)$ corresponds to a configuration in which every vertex of the undirected graph $\mathcal{G}_b = (\mathcal{V}, \mathcal{E}_b)$ is embedded as a point in an Euclidean space. Here, $\mathcal{G}_b$ serves as the interaction topology that encodes inter-agent communication links. The vector $q = \left[q_1^T, \ldots, q_n^T\right]^T \in \mathbb{R}^{dn}$ specifies the overall positions of all agents, where each $q_i \in \mathbb{R}^d$ denotes the position of agent i in d dimensions.

Under the assumption $q_i \neq q_j$, the vector along the directed edge (i, j) is defined as follows:

$$e_{ij} := q_j - q_i, \tag{5}$$

and the corresponding unit vector, representing the bearing, is provided by the following:

$$g_{ij} := \frac{e_{ij}}{\|e_{ij}\|}. \tag{6}$$

It follows from (6) that g_{ij} is a unit vector that shares the same direction as the relative position vector e_{ij}, which encodes the bearing of agent j, as seen from agent i. The matrix $P_{g_{ij}} = I_d - g_{ij}g_{ij}^T$ serves as the orthogonal projection operator onto the subspace perpendicular to g_{ij}, where $I_d \in \mathbb{R}^{d\times d}$ denotes the identity matrix. This projection matrix is symmetric, idempotent, and positive semi-definite, with eigenvalues $\{0, 1, \ldots, 1\}$, and its null space is spanned by g_{ij}. Consequently, a vector $x \in \mathbb{R}^d$ lies in the direction of g_{ij} if and only if $P_{g_{ij}}x = 0$.

To orient an undirected graph means to assign a distinct direction to every one of its edges. An oriented graph is defined as the result of combining an undirected graph with a selected directionality for its edges. In this study, we take into account a randomly chosen oriented version of the graph $\mathcal{G}$. Let m stand for the overall count of undirected edges in the interaction graph $\mathcal{G}$. When the graph is assigned an arbitrary but fixed orientation, each undirected edge corresponds to one directed edge, resulting in a total of m directed edges in the oriented graph. For each undirected edge (i, j) in $\mathcal{G}$, we assign it a unique index $k \in \{1, \ldots, m\}$, corresponding to a directed edge from agent i to agent j in the oriented graph. The edge vector $e^k \in \mathbb{R}^d$ and the corresponding bearing vector $g^k \in \mathbb{R}^d$ associated with the k-th directed edge are defined as follows:

$$e_k := e_{ij} = q_j - q_i, g_k := \frac{e_k}{\|e_k\|}. \tag{7}$$

Define the concatenated vectors $e \triangleq \mathrm{col}(e_1, \ldots, e_m)$ and $g \triangleq \mathrm{col}(g_1, \ldots, g_m)$. The oriented graph's connectivity is encoded in the incidence matrix $E \in \mathbb{R}^{m\times n}$. The incidence matrix E encodes directed edge relationships through its sign convention: for the k-th edge connecting vertices i and j, the matrix element $[E]_{ki}$ assumes a value of -1 indicating vertex i as the edge-originating source node, while the corresponding element $[E]_{kj}$ takes a value of $+1$ designating vertex j as the edge-terminating sink node, thereby establishing the fundamental directional relationship between adjacent vertices in the oriented graph structure. All remaining elements in the k-th row take the value zero, given that these vertices have no incidence relation with edge k. This construction ensures that E encodes the orientation of the graph edges in relation to the vertices. Therefore, the following definition is obtained:

$$e = (E \otimes I_d)q := \bar{E}q, \tag{8}$$

where the symbol $\otimes$ represents the Kronecker product. Let $1_n = [1, \ldots, 1]^T \in \mathbb{R}^n$. In the case of a connected graph, the relation $E1_n = 0$ holds, and the rank of E is $n - 1$ [39].

Lemma 3 ([36]). *Given each agent's capacity to acquire relative bearing measurements from a local subset of adjacent agents, and that the structure of these measurements is governed by $\mathcal{G}_b$, the following inequality can be established:*

$$\|e_k\| \leq 2s\sqrt{n-1}, \forall k = 1, \ldots, n, \tag{9}$$

where s denotes configuration scaling. The rigorous proof is omitted here since relevant details can be found in Corollary 2 of ref. [20].

Lemma 4 ([26]). *A graph $\mathcal{G}$ is infinitesimally bearing rigid if and only if the null space of its bearing rigidity matrix $\mathcal{R}(q)$ comprises precisely the linear span of two fundamental subspaces: the range space of the Kronecker product $1_n \otimes I_d$ (representing translational motions) and the*

displacement vector $q - 1_n \otimes \bar{q}$ *(encoding scaling transformations). Here, the configuration centroid* $\bar{q}$ *is computed as the arithmetic mean of all agent positions:*

$$\bar{q} = (1/n)\sum_{i=1}^{n} q_i = (1/n)(1_n \otimes I_d)^T q. \tag{10}$$

2.4. Gram–Schmidt Process (GSP)

Considering a collection of r linearly independent vectors $\mathcal{W} = \{w_1, w_2, \ldots, w_d\} \subset \mathbb{R}^r$, the Gram–Schmidt orthonormalization procedure constructs an orthonormal basis $\{p_1, p_2, \ldots p_r\}$ through the following recursive process:

$$\begin{aligned} v_1 &:= w_1, p_1 := v_1/\|v_1\|, \\ v_2 &:= w_2 - \langle w_2, p_1\rangle p_1, p_2 := v_2/\|v_2\|, \\ &\vdots \\ v_r &:= w_r - \sum_{k=1}^{r-1} \langle z_r, p_k\rangle p_k, p_r := \alpha_0 v_r/\|v_r\|. \end{aligned} \tag{11}$$

Here, $\langle \cdot, \cdot \rangle$ represents the standard inner product. To ensure that the resulting orthonormal matrix $D = [q_1, q_2, \ldots q_d]$ satisfies $\det(D) = 1$, the scalar coefficient α_0 is introduced in the final step and defined as follows:

$$\alpha_0 := \operatorname{sign}\big(\det\big([p_1, \ldots, p_{d-1}, v_d/\|v_d\|]\big)\big), \tag{12}$$

where v_d is the last intermediate vector before normalization, and $\operatorname{sign}(\cdot)$ denotes the sign function. The GSP will be extensively used in this paper to build an auxiliary matrix of the orientation of the agents.

2.5. Target Formation

The following serves as the definition of the intended target formation.

Definition 3. *If all agents satisfy the prescribed relative bearings between neighbors, as defined by* $\left\{g_{ij}^*\right\}_{(i,j)\in\mathcal{E}}$*, the formation is said to have achieved the desired shape. The leaders move at a constant velocity* $v_c \in \mathbb{R}^d$*.*

The intended configuration is regulated through invariant inter-agent bearings and leader dynamics, exhibiting two critical attributes. First, formation realizability requires admissible bearing-leader configurations that guarantee existence. These feasible solutions derive directly from formations possessing the target geometric structure.

Second, formation uniqueness necessitates specific algebraic conditions characterized by the bearing Laplacian $\mathcal{A} \in \mathbb{R}^{dn\times dn}$. The entries of $\mathcal{A}$ are constructed as follows:

1. For off-diagonal blocks, if agent i is not connected to agent j, i.e., $(i, j) \notin \mathcal{E}$, then the corresponding block is the zero matrix:

$$[\mathcal{A}]_{ij} = 0_{d\times d}. \tag{13}$$

2. If agent i and j are connected, i.e., $(i, j) \in \mathcal{E}$, then the off-diagonal block is provided by the negative projection matrix along the desired bearing g_{ij}^*:

$$[\mathcal{A}]_{ij} = -P_{g_{ij}^*}. \tag{14}$$

3. For the diagonal blocks, i.e., when $i = j$, the corresponding block aggregates the contributions from all neighbors of agent i, specifically constituting the summation of the projection matrices over its neighbor set $\mathcal{N}_i$:

$$[\mathcal{A}]_{ij} = \sum_{k\in\mathcal{N}_i} P_{g_{ik}^*}. \tag{15}$$

Functioning as a weighted Laplacian, $\mathcal{A}$ jointly encodes the graph topology and target formation bearings within a unified algebraic framework. For undirected graphs, $\mathcal{A}$ exhibits three fundamental algebraic properties:

1. Symmetric positive semi-definiteness.
2. Kernel containment: The null space subsumes all vectors formed by global translations of the target configuration q^* and joint rotations of the agent ensemble.
3. $\text{rank}(\mathcal{A}) = dn - d - 1$ under generic configurations.

Based on the partition of agents into leaders and followers, the matrix $\mathcal{A}$ can be further partitioned into sub-matrices corresponding to the following groups:

$$\mathcal{A} = \begin{bmatrix} \mathcal{A}_{ll} & \mathcal{A}_{lf} \\ \mathcal{A}_{fl} & \mathcal{A}_{ff} \end{bmatrix}. \tag{16}$$

The bearing Laplacian rigorously encodes sufficient and necessary criteria for target formation uniqueness, formally established below.

Lemma 5 ([21]). *The desired configuration $q^*(t) \in \mathbb{R}^{dn}$, representing the stacked position vectors of all agents, is uniquely defined by a set of target-bearing $\left\{g_{ij}^*\right\}_{(i,j)\in\mathcal{E}}$ and the known positions of the leader agent $\left\{q_i^*\right\}_{i\in\mathcal{V}_l}$, if and only if the submatrix $\mathcal{A}_{ff}$ of the bearing Laplacian, corresponding to follower–follower interactions, is invertible.*

When $\mathcal{A}_{ff}$ is nonsingular, the kinematic states (positions/velocities) of the following agents within the target configuration are uniquely determined by the leader states:

$$\begin{aligned} q_f^*(t) &= -\mathcal{A}_{ff}^{-1}\mathcal{A}_{fl}q_l^*(t), \\ v_f^*(t) &= -\mathcal{A}_{ff}^{-1}\mathcal{A}_{fl}v_l^*(t), \end{aligned} \tag{17}$$

where $q_l^*(t) \in \mathbb{R}^{dn_l}$ and $v_l^*(t) \in \mathbb{R}^{dn_l}$ denote the dynamic leader reference signals for position and velocity states, respectively. Throughout this work, leaders maintain identical velocity profiles characterized by a common constant vector v_c, such that $v_l^*(t) = 1_n \otimes v_c$.

To guarantee the uniqueness of the intended configuration, it is essential that the system includes a sufficient number of appropriately selected leaders. In particular, the presence of no fewer than two leaders is a fundamental requirement to uniquely define the target configuration. For further details on leader selection, please refer to [26].

3. Main Results

Assume a multi-agent system composed of n agents operating within a d-dimensional Euclidean space, where the spatial dimension satisfies $d \in \{2, 3\}$. Each agent operates within its own local coordinate system, which remains fixed relative to its body, and no global reference frame is shared among the agents. The dynamics of agent i follows a standard double-integrator model, and the disturbance $d_{v_i^B}$ is presumed to be uniformly bounded over time; that is, there exists a constant $\bar{d}_i > 0$ satisfying $\left\|d_{v_i^B}\right\| \leq \bar{d}_i$ for all $t \geq 0$. The model is formulated as follows:

$$\dot{q}_i^B(t) = v_i^B, \dot{v}_i^B(t) = u_i^B + d_{v_i^B}. \tag{18}$$

Here, vectors $q_i^B, v_i^B, u_i^B \in \mathbb{R}^d$ represent the spatial location, velocity, and acceleration command of agent i, respectively. The term $d_{v_i^B}$ represents an external disturbance term

acting on agent i. All quantities are described relative to the agent's own body-fixed reference frame ${}^{i}\mathcal{F}$. It is worth noting that the double-integrator model, as formulated in Equation (14), focuses solely on linear velocity and acceleration, and the angular velocity mentioned below is only considered in the context of estimating the agents' orientations. This system model is widely adopted in the fields of multi-agent navigation and formation control due to its simplicity and analytical tractability. Investigating extensions to more complex agent dynamics is left for subsequent research.

The global orientation of agent i is described by an orthogonal matrix D_i. Each column of D_i corresponds to a unit vector defining the orientation of agent i's body-fixed frame with respect to the global coordinate system $\mathcal{F}$. Thus, D_i functions as a rotation matrix that transforms quantities described in $\mathcal{F}$ into representations in agent i's own reference frame, denoted as ${}^{i}\mathcal{F}$. For all agents, let D_k denote their respective orientations. The orientation of agent j's body-fixed frame relative to that of agent i is characterized by the following transformation:

$$D_{ij} = D_i^{-1} D_j = D_i^T D_j. \tag{19}$$

$\mathcal{G}_o = (\mathcal{V}, \mathcal{E}_o)$ being undirected serves to characterize the relative orientation measurement structure among agents. The presence of edge $(i, j) \in \mathcal{E}_o$ encodes the availability of relative orientation data D_{ij} to agent i. Based on such measurements from its neighbors $k \in \mathcal{N}_i$, agent i computes an estimate of its own orientation, denoted by $\hat{D}_i \in SO(d)$. Furthermore, for each $(i, j) \in \mathcal{E}_o$, agent j also transmits a supporting matrix to agent i, which is formally described in the next subsection. Consequently, $\mathcal{G}_o$ functions not only as a sensing topology but also as a communication network. The Laplacian matrix associated with $\mathcal{G}_o$ is denoted by $\mathcal{L}_o$.

Up to this point, two separate interaction graphs have been introduced: $\mathcal{G}_o$, governing orientation estimation, and $\mathcal{G}_b$, responsible for formation control. This study primarily aims to develop an orientation estimation scheme that guarantees convergence within a fixed time.

3.1. Fixed-Time Orientation Estimation Law

To facilitate orientation estimation, each agent i is associated with a supporting matrix $\mathcal{Y}_i \in \mathbb{R}^{d \times d}$. To obtain $\hat{D}_i$, the estimated orientation, the matrix $\mathcal{Y}_i$ is processed using the GSP, as outlined in [31]:

$$\hat{D}_i^T = GSP\left(\mathcal{Y}_i^T\right). \tag{20}$$

This procedure ensures that $\hat{D}_i(t)$ remains orthogonal and lies in the special orthogonal group $SO(d)$, as required for valid rotation matrices.

To capture the evolution of each $\mathcal{Y}_i(t)$, the following distributed estimation scheme is formulated:

$$\begin{aligned} \dot{\mathcal{Y}}_i(t) = & -\mathcal{Y}_i(t)\left(\left(\sigma_i^B\right)^{\times}\right)^T \\ & + \sum_{j \in \mathcal{N}_i} \frac{\mathcal{Y}_j(t) D_{ij}^T(t) - \mathcal{Y}_i(t)}{\left\| \mathcal{Y}_j D_{ij}^T - \mathcal{Y}_i \right\|_F^{\alpha_1}} \\ & + \sum_{j \in \mathcal{N}_i} \left(\mathcal{Y}_j(t) D_{ij}^T(t) - \mathcal{Y}_i(t)\right) \left\| \mathcal{Y}_j D_{ij}^T - \mathcal{Y}_i \right\|_F^{\alpha_1} \end{aligned}, \tag{21}$$

where $\alpha_1 \in (0,1)$ is a design parameter, and $\sigma_i^B \in \mathbb{R}^d$ denotes the angular velocity of agent i, expressed in its own body-fixed coordinate frame ${}^i\mathcal{F}$. The Frobenius norm $\|\cdot\|_F$, which quantifies the Euclidean distance between matrices, is defined as follows:

$$\|\mathcal{Z}-\mathcal{H}\|_F = \sqrt{tr\Big\{(\mathcal{Z}-\mathcal{H})^T(\mathcal{Z}-\mathcal{H})\Big\}}. \tag{22}$$

The operator $(\cdot)^\times$ denotes the matrix representation of the cross product in skew-symmetric form, which for vectors in $\mathbb{R}^3$, is provided by the following:

$$\sigma^\times = \begin{bmatrix} 0 & -\sigma_z & \sigma_y \\ \sigma_z & 0 & -\sigma_x \\ -\sigma_y & \sigma_x & 0 \end{bmatrix}. \tag{23}$$

As the estimation law (20) is designed to ensure fixed-time convergence of the orientation estimates, the analysis focuses on the limiting behavior of each supporting matrix $\mathcal{Y}_i$ for all $i \in \mathcal{V}$. As a result, no assumptions are imposed on the initial conditions of $\mathcal{Y}_i$; the transient response is not of primary interest. Instead, attention is focused on the final orientations once the estimation dynamics have been stabilized.

At any time t, the orientation estimate $\hat{D}_i(t)$ can be obtained by applying the GSP to $\mathcal{Y}_i(t)$. This operation is computationally efficient, involving a limited number of operations, approximately proportional to $O(d^3)$. It is assumed that the evaluation of $\hat{D}_i(t)$ incurs negligible delay. Notably, the GSP is applied only after the auxiliary matrix $\mathcal{Y}_i(t)$ has reached its steady state, as will be rigorously demonstrated in the next section.

Theorem 1. *Under the proposed estimation scheme, the fixed-time global convergence of $\hat{D}_i$ to $D^c D_i$ is achieved for almost every initial condition, with the exception of a measure-zero set due to potential GSP degeneracy.*

Proof. The estimation law (20) is equivalently transformed into the following:

$$\begin{aligned}
\dot{\mathcal{Y}}_i(t)D_i^T(t) &= -\mathcal{Y}_i(t)\Big(\big(\sigma_i^B\big)^\times\Big)^T D_i^T(t) + \sum_{j\in\mathcal{N}_i}\frac{\mathcal{Y}_j(t)D_{ij}^T(t)-\mathcal{Y}_i(t)}{\big\|\mathcal{Y}_jD_{ij}^T-\mathcal{Y}_i\big\|_F^{\alpha_1}}D_i^T(t)\\
&\quad+\sum_{j\in\mathcal{N}_i}\Big(\mathcal{Y}_j(t)D_{ij}^T(t)-\mathcal{Y}_i(t)\Big)\big\|\mathcal{Y}_jD_{ij}^T-\mathcal{Y}_i\big\|_F^{\alpha_1}D_i^T(t)\\
&= -\mathcal{Y}_i(t)\Big(\big(\sigma_i^B\big)^\times\Big)^T D_i^T(t) + \sum_{j\in\mathcal{N}_i}\frac{\mathcal{Y}_j(t)D_i^T(t)-\mathcal{Y}_i(t)D_j^T}{\big\|\mathcal{Y}_jD_{ij}^T-\mathcal{Y}_i\big\|_F^{\alpha_1}}D_i^T(t)\\
&\quad+\sum_{j\in\mathcal{N}_i}\Big(\mathcal{Y}_j(t)D_i^T(t)-\mathcal{Y}_i(t)D_j^T\Big)\big\|\mathcal{Y}_jD_{ij}^T-\mathcal{Y}_i\big\|_F^{\alpha_1}D_i^T(t)\\
&= -\mathcal{Y}_i(t)\Big(\big(\sigma_i^B\big)^\times\Big)^T D_i^T(t) + \sum_{j\in\mathcal{N}_i}\frac{\mathcal{Y}_j(t)D_j^T(t)-\mathcal{Y}_i(t)D_i^T(t)}{\big\|\mathcal{Y}_jD_{ij}^T-\mathcal{Y}_i\big\|_F^{\alpha_1}}\\
&\quad+\sum_{j\in\mathcal{N}_i}\Big(\mathcal{Y}_j(t)D_j^T(t)-\mathcal{Y}_i(t)D_i^T(t)\Big)\big\|\mathcal{Y}_jD_{ij}^T-\mathcal{Y}_i\big\|_F^{\alpha_1}
\end{aligned}. \tag{24}$$

Let us consider the decomposition $\mathcal{Y}_i(t) = \mathcal{T}_i(t)D_i(t)$, where $\mathcal{T}_i(t)$ denotes a supporting matrix associated with agent i. It is important to emphasize the following:

$$\dot{\mathcal{T}}_i = \frac{d(\mathcal{Y}_iD_i^T)}{dt} = \dot{\mathcal{Y}}_iD_i^T + \mathcal{Y}_i\Big(\big(\sigma_i^B\big)^\times\Big)^T D_i^T. \tag{25}$$

Thus, the former equation can be reformulated as follows:

$$\dot{\mathcal{T}}_i(t) = \sum_{j\in\mathcal{N}_i}\left(\frac{(\mathcal{T}_j-\mathcal{T}_i)}{\|\mathcal{T}_i-\mathcal{T}_j\|_F^{\alpha_1}} + (\mathcal{T}_j-\mathcal{T}_i)\|\mathcal{T}_i-\mathcal{T}_j\|_F^{\alpha_1}\right). \tag{26}$$

Define the stacked matrix $\mathcal{T} = \left[\mathcal{T}_1^T,\ldots,\mathcal{T}_n^T\right]^T \in \mathbb{R}^{dn\times d}$, where each block $\mathcal{T}_i \in \mathbb{R}^{d\times d}$ corresponds to the transformed supporting matrix associated with agent i. This formulation collects all agents' transformed matrices into a unified structure. With this notation, Equation (25) can be reformulated as follows:

$$\dot{\mathcal{T}}(t) = -(\bar{\mathcal{L}}_o \otimes I_d)\mathcal{T}(t). \tag{27}$$

The orientation interaction graph $\mathcal{G}_o$ induces a weighted Laplacian $\bar{\mathcal{L}}_o$ whose matrix elements are specified as follows:

1. For any two distinct nodes i and j, if there is no edge between them (i.e., $(i,j)\in\mathcal{E}_o$), or if the corresponding orientation matrices are identical (i.e., $\mathcal{T}_i = \mathcal{T}_j$), the corresponding entry of the matrix satisfies the following:

$$[\mathcal{L}]_{ij} = 0. \tag{28}$$

2. When an edge exists between agents i and j (i.e., $(i,j)\in\mathcal{E}_o$), and their orientation matrices are not equal (i.e., $\mathcal{T}_i \neq \mathcal{T}_j$), the off-diagonal entry is defined by a combination of inverse and direct Frobenius norm terms:

$$[\mathcal{L}]_{ij} = -\frac{1}{\|\mathcal{T}_i-\mathcal{T}_j\|_F^{\alpha_1}} - \|\mathcal{T}_i-\mathcal{T}_j\|_F^{\alpha_1}. \tag{29}$$

3. The diagonal elements of the Laplacian matrix (i.e., when $i=j$) are computed as the sum of the corresponding row's off-diagonal entries, ensuring each row sums to zero:

$$[\mathcal{L}]_{ij} = \sum_{k\in\mathcal{N}_i}[\mathcal{L}]_{ik}, \forall i\in\mathcal{V}. \tag{30}$$

Let $\mathcal{T}^c = \frac{1}{n}(1_n\otimes I_d)^T\mathcal{T}(t)$ denote the average of the stacked matrix $\mathcal{T}(t)$, and define each agent's deviation from this average as $\mathcal{T}_i(t) = \mathcal{T}^c + \varsigma_i(t)$. Collectively, the deviation vectors for all agents are assembled into a single stacked vector defined as $\varsigma(t) = \left[\varsigma_1^T,\ldots,\varsigma_n^T\right]^T$. Since $(1_n\otimes I_d)^T\dot{\mathcal{T}}(t) = -(1_n\otimes I_d)^T(\bar{\mathcal{L}}_o\otimes I_d)\mathcal{T}(t) = 0$, the average matrix remains constant over time. Consequently, the time derivative of the deviation $\varsigma_i(t)$ equals the identical differential operator applied to $\mathcal{T}_i(t)$.

To establish closed-loop stability, consider the quadratic Lyapunov function candidate:

$$V(t) = \left(\frac{1}{2}\right)\sum_{i=1}^{n}\|\varsigma_i\|_F^2 = \left(\frac{1}{2}\right)\sum_{i=1}^{n} tr\left(\varsigma_i^T\varsigma_i\right). \tag{31}$$

The temporal derivative of the Lyapunov function yields the following:

$$\begin{aligned}
\dot{V}(t) &= \sum_{i=1}^{n} tr\left(\varsigma_i^T \dot{\varsigma}_i\right) \\
&= -tr\left\{\sum_{i=1}^{n} \varsigma_i^T \sum_{j\in\mathcal{N}_i} \left(\frac{(\varsigma_i-\varsigma_j)}{\|\varsigma_i-\varsigma_j\|_F^{\alpha_1}} + (\varsigma_i-\varsigma_j)\|\varsigma_i-\varsigma_j\|_F^{\alpha_1}\right)\right\}, \\
&= -tr\left\{\sum_{(i,j)\in\mathcal{E}_o} \left(\varsigma_i^T-\varsigma_j^T\right)\left(\frac{(\varsigma_i-\varsigma_j)}{\|\varsigma_i-\varsigma_j\|_F^{\alpha_1}} + (\varsigma_i-\varsigma_j)\|\varsigma_i-\varsigma_j\|_F^{\alpha_1}\right)\right\}, \\
&= -\sum_{(i,j)\in\mathcal{E}_o}\left(\frac{\|\varsigma_i-\varsigma_j\|_F^2}{\|\varsigma_i-\varsigma_j\|_F^{\alpha_1}} + \|\varsigma_i-\varsigma_j\|_F^2\|\varsigma_i-\varsigma_j\|_F^{\alpha_1}\right), \\
&= -\sum_{(i,j)\in\mathcal{E}_o}\left(\left(\|\varsigma_i-\varsigma_j\|_F^2\right)^{(2-\alpha_1)/2} + \left(\|\varsigma_i-\varsigma_j\|_F^2\right)^{(2+\alpha_1)/2}\right), \\
&\le -\left(\sum_{(i,j)\in\mathcal{E}_o}\|\varsigma_i-\varsigma_j\|_F^2\right)^{(2-\alpha_1)/2} - n^{1-(2+\alpha_1)/2}\left(\sum_{(i,j)\in\mathcal{E}_o}\|\varsigma_i-\varsigma_j\|_F^2\right)^{(2+\alpha_1)/2}, \\
&\le -\left(tr\left\{\sum_{(i,j)\in\mathcal{E}_o}\left(\varsigma_i^T-\varsigma_j^T\right)(\varsigma_i-\varsigma_j)\right\}\right)^{(2-\alpha_1)/2}, \\
&\quad - n^{1-(2+\alpha_1)/2}\left(tr\left\{\sum_{(i,j)\in\mathcal{E}_o}\left(\varsigma_i^T-\varsigma_j^T\right)(\varsigma_i-\varsigma_j)\right\}\right)^{(2+\alpha_1)/2}.
\end{aligned} \tag{32}$$

As concluded from Lemma 2, with $\mathcal{L}_o$ denoting the Laplacian matrix of $\mathcal{G}_o$, the inequality can be expressed as follows:

$$\dot{V}(t) \le -\left(tr\left\{\varsigma^T(\mathcal{L}_o\otimes I_d)\varsigma\right\}\right)^{(2-\alpha_1)/2} - n^{1-(2+\alpha_1)/2}\left(tr\left\{\varsigma^T(\mathcal{L}_o\otimes I_d)\varsigma\right\}\right)^{(2+\alpha_1)/2}. \tag{33}$$

The Kronecker product $\mathcal{L}_o\otimes I_d$ possesses precisely d zero eigenvalues, with its null space constituting the linear subspace spanned by the range of the matrix $1_n\otimes I_d$, a geometric representation of all possible translational motions of the multi-agent formation in d-dimensional space. Each column $[\varsigma]_k$ of the matrix ς satisfies the inequality below:

$$[\varsigma]_k^T(\mathcal{L}_o\otimes I_d)[\varsigma]_k \ge \theta_{d+1}[\varsigma]_k^T[\varsigma]_k, \tag{34}$$

where θ_{d+1} denotes the minimal positive element among the eigenvalues of the Kronecker product $\mathcal{L}_o\otimes I_d$. Substituting this inequality into Equation (26) yields the following result:

$$\begin{aligned}
\dot{V}(t) &\le -\left(\theta_{d+1}\sum_{k=1}^{d}\|[\varsigma]_k\|^2\right)^{(2-\alpha_1)/2} - n^{1-(2+\alpha_1)/2}\left(\theta_{d+1}\sum_{k=1}^{d}\|[\varsigma]_k\|^2\right)^{(2+\alpha_1)/2} \\
&\le -\theta_{d+1}^{(2-\alpha_1)/2}\left(\sum_{k=1}^{d}\|[\varsigma]_k\|^2\right)^{(2-\alpha_1)/2} - n^{1-(2+\alpha_1)/2}\theta_{d+1}^{(2+\alpha_1)/2}\left(\sum_{k=1}^{d}\|[\varsigma]_k\|^2\right)^{(2+\alpha_1)/2} \\
&\le -\theta_{d+1}^{(2-\alpha_1)/2}\left(\sum_{k=1}^{d} tr\left(\varsigma_i^T\varsigma_i\right)\right)^{(2-\alpha_1)/2} - n^{1-(2+\alpha_1)/2}\theta_{d+1}^{(2+\alpha_1)/2}\left(\sum_{k=1}^{d} tr\left(\varsigma_i^T\varsigma_i\right)\right)^{(2+\alpha_1)/2} \\
&\le -\theta_{d+1}^{(2-\alpha_1)/2}(2V(t))^{(2-\alpha_1)/2} - n^{1-(2+\alpha_1)/2}\theta_{d+1}^{(2+\alpha_1)/2}(2V(t))^{(2+\alpha_1)/2} \\
&\le -\kappa_1 V(t)^{(2-\alpha_1)/2} - \kappa_2 V(t)^{(2+\alpha_1)/2}.
\end{aligned} \tag{35}$$

Here, the constantsare defined as $\kappa_1 = (2\theta_{d+1})^{(2-\alpha_1)/2}$ and $\kappa_2 = n^{1-(2+\alpha_1)/2}(2\theta_{d+1})^{(2-\alpha_1)/2}$. Leveraging Lemma 1 together with Equation (30), it can be concluded that $V(t)$ reaches zero within a fixed time. Furthermore, the settling time is bounded above by $T_{\max} = \pi/(\alpha_1\sqrt{\kappa_1\kappa_2})$. This implies that all matrices $\mathcal{T}_i(t)$ for every $i\in\mathcal{V}$ converge globally to the common value $\mathcal{T}_c$ within a fixed time. Consequently, each estimated orientation $\hat{D}_i(t)$ approaches $D^cD_i, \forall i = 1,\ldots,n$, where D^c is obtained by ap-

plying the GSP to $\mathcal{T}_c$. Consequently, the true orientation states of all agents converge to their actual values within a fixed time, with estimation accuracy bound by network-wide constant rotation D^c. □

3.2. Fixed-Time Bearing-Only Formation Control

Once the estimated orientations $\hat{D}_i$ have achieved the actual orientations, we present the fixed-time formation control problem in formal terms. This bearing-based control strategy enforces formation shape convergence within a fixed time without global coordinate awareness, leveraging distributed estimators that provide rigorous orientation estimates with fixed-time convergence. Thus, this part proposes an almost global fixed-time control strategy based solely on bearing measurements for formation stabilization.

A virtual control input for agent i is defined as follows:

$$\hat{v}_i^B = -\sum_{j\in\mathcal{N}_i}\left(P_{g_{ij}^B}\hat{D}_i^T \operatorname{sig}\left(\hat{D}_i P_{g_{ij}^B}\hat{D}_i^T g_{ij}^*\right)^{\tau} + P_{g_{ij}^B}\hat{D}_i^T \operatorname{sig}\left(\hat{D}_i P_{g_{ij}^B}\hat{D}_i^T g_{ij}^*\right)^{\rho}\right), \tag{36}$$

where $\tau = 1-(1/\mu), \rho = 1+(1/\mu), \mu > 1$ are positive constant coefficients, function $\operatorname{sig}(\cdot)$ is defined as $\operatorname{sig}(\varphi)^{\tau} = [\operatorname{sign}(\varphi_1)|\varphi_1|^{\tau}, \ldots, \operatorname{sign}(\varphi_d)|\varphi_d|^{\tau}]$, and $\hat{D}_i$ is the orientation estimated by the observer outlined earlier. The derivative of the virtual input $\hat{v}_i^B$ can be obtained as follows:

$$\begin{aligned}\dot{\hat{v}}_i^B = -\dot{\hat{D}}_i^T \sum_{j\in\mathcal{N}_i}\Bigg\{&\left(-\frac{\dot{g}_{ij}g_{ij}^T + g_{ij}\dot{g}_{ij}^T}{\|g_{ij}\|^2} + 2\frac{\left(g_{ij}^T\dot{g}_{ij}\right)g_{ij}g_{ij}^T}{\|g_{ij}\|^4}\right)\varpi_{ij}\\ &+P_{g_{ij}}\cdot\vartheta_{ij}\cdot\left(-\frac{\dot{g}_{ij}g_{ij}^T + g_{ij}\dot{g}_{ij}^T}{\|g_{ij}\|^2} + 2\frac{\left(g_{ij}^T\dot{g}_{ij}\right)g_{ij}g_{ij}^T}{\|g_{ij}\|^4}\right)g_{ij}^*\Bigg\},\end{aligned} \tag{37}$$

where $\varpi_{ij} = \operatorname{sig}\left(P_{g_{ij}}g_{ij}^*\right)^{\tau} + \operatorname{sig}\left(P_{g_{ij}}g_{ij}^*\right)^{\rho}$, $s_{ij} = P_{g_{ij}}g_{ij}^*$, and the Jacobian matrix is defined as follows:

$$\vartheta_{ij} = \frac{\partial\varpi_{ij}}{\partial s_{ij}} = \operatorname{diag}\left(\tau|s_{ij,1}|^{\tau-1} + \rho|s_{ij,1}|^{\rho-1}, \tau|s_{ij,2}|^{\tau-1} + \rho|s_{ij,2}|^{\rho-1}, \cdots\right). \tag{38}$$

We define the velocity tracking error as $e_{v_i^B} = \hat{v}_i^B - v_i^B$, where v_i^B is the actual velocity of agent i. According to fixed-time control theory [34], the terminal sliding mode outer-loop controller can be constructed to guarantee that the velocity tracking error $e_{v_i^B}$ reaches zero within a fixed time, and it is presented below:

$$u_i^B = \kappa_3 \operatorname{sig}\left(e_{v_i^B}\right)^{1-(1/2\gamma)} + \kappa_4 \operatorname{sig}\left(e_{v_i^B}\right)^{1+(1/2\gamma)} + \kappa_5 \operatorname{sgn}\left(e_{v_i^B}\right) + \dot{\hat{v}}_i^B, \tag{39}$$

where $\kappa_3, \kappa_4, \kappa_5$ are strictly positive constants with $\gamma > 1$, and $\operatorname{sgn}(\cdot)$ is the sign function used to robustly handle bound external disturbances $d_{v_i^B}$. The gain κ_5 is chosen such that $\kappa_5 > \left\|d_{v_i^B}\right\|$. Within the global system, the continuous-time dynamics of agent i are characterized as follows:

$$\dot{q}_i = D_i v_i^B, \dot{v}_i^B = u_i^B + d_{v_i^B}\ \forall i \in \mathcal{V}. \tag{40}$$

For outer-loop stability certification, the Lyapunov function candidate adopts the following form:

$$V(t) = (1/2)\sum_{i=1}^{n} e_{v_i^B}^T e_{v_i^B}. \tag{41}$$

Differentiating the preceding equation with respect to time yields the following:

$$\begin{aligned}\dot{V}(t) &= \sum_{i=1}^{n} e_{v_i^B}^T \left(\dot{\hat{v}}_i^B - u_i^B - d_{v_i^B}\right) \\ &\leq -\kappa_3 V^{\alpha_2} - \kappa_4 V^{\alpha_3} - \sum_{i=1}^{n} \kappa_5 \left\| e_{v_i^B} \right\| + \sum_{i=1}^{n} \left\| e_{v_i^B} \right\| \left\| d_{v_i^B} \right\|,\end{aligned} \tag{42}$$

where $\alpha_2 = (4\gamma - 1)/4\gamma$, $\alpha_3 = (4\gamma + 1)/4\gamma$. Therefore, the inequality $\dot{V}(t) \leq -\kappa_3 V^{\alpha_2} - \kappa_4 V^{\alpha_3}$ holds; hence, the velocity v_i^B in body-fixed frame can track the desired virtual velocity $\hat{v}_i^B$ in a fixed time according to Lemma 1.

The following proof shows that the position error e_{p_i} associated with the formation vanishes within a fixed time. Equation (31) reveals that the local projection matrix admits the coordinate transformation: $P_{g_{ij}^B} = I_d - g_{ij}^B \left(g_{ij}^B\right)^T = D_i^T P_{g_{ij}} D_i$, where g_{ij}^B represents the relative bearing g_{ij} expressed in the i-th coordinate frame. Crucially, the orientation estimate achieves the relation $\hat{D}i \equiv D^c Di$, $\forall i \in \mathcal{V}$ for $t \geq T_o$, with T_o denoting the predefined-time convergence upper limit for the distributed estimation scheme in the above section. Therefore, substituting $\hat{D}_i = D^c D_i$ and the virtual input $\hat{v}_i^B$ into the dynamics yields the following:

$$\begin{aligned}\dot{q}_i &= -D_i \textstyle\sum_{j \in \mathcal{N}_i} \left(D_i^T P_{g_{ij}} D_i \hat{D}_i^T \operatorname{sig}\left(\hat{D}_i D_i^T P_{g_{ij}^B} D_i \hat{D}_i^T g_{ij}^* \right)^{\tau} \right. \\ &\quad \left. + D_i^T P_{g_{ij}} D_i \hat{D}_i^T \operatorname{sig}\left(\hat{D}_i D_i^T P_{g_{ij}^B} D_i \hat{D}_i^T g_{ij}^* \right)^{\rho} \right) \\ &= -\textstyle\sum_{j \in \mathcal{N}_i} P_{g_{ij}} (D^c)^T \left(\operatorname{sig}\left(D^c P_{g_{ij}} (D^c)^T g_{ij}^* \right)^{\tau} \right. \\ &\quad \left. + \operatorname{sig}\left(D^c P_{g_{ij}} (D^c)^T g_{ij}^* \right)^{\rho} \right) \\ &= -\textstyle\sum_{j \in \mathcal{N}_i} P_{g_{ij}} (D^c)^T \left(\operatorname{sig}\left(D^c P_{g_{ij}} g_{ij}^c \right)^{\tau} + \operatorname{sig}\left(D^c P_{g_{ij}} g_{ij}^c \right)^{\rho} \right)\end{aligned} \tag{43}$$

where $g_{ij}^c = (D^c)^T g_{ij}^*$ represents the desired bearing. We denote stacked vectors as $g^c = \left[g_1^c, \ldots, g_m^c\right]^T \in \mathbb{R}^{dm}$; accordingly, the control law for formation can be formulated in a compact expression as follows:

$$\dot{q} = \bar{E}^T \operatorname{diag}\left(P_{g_k} (D^c)^T \right) \left(\operatorname{sig}\left(\operatorname{diag}\left(D^c P_{g_k} \right) g^c \right)^{\tau} + \operatorname{sig}\left(\operatorname{diag}\left(D^c P_{g_k} \right) g^c \right)^{\rho} \right). \tag{44}$$

Given constant–velocity leader dynamics, the follower coordination law is enhanced as follows:

$$\begin{aligned}\dot{q} = \bar{E}^T \operatorname{diag}\left(P_{g_k} (D^c)^T \right) \left(\operatorname{sig}\left(\operatorname{diag}\left(D^c P_{g_k} \right) g^c \right)^{\tau} \right. \\ \left. + \operatorname{sig}\left(\operatorname{diag}\left(D^c P_{g_k} \right) g^c \right)^{\rho} \right) - \mathcal{A}_{ff}^{-1} \mathcal{A}_{fl} v_l^*(t),\end{aligned} \tag{45}$$

where $v_f^*(t) = -\mathcal{A}_{ff}^{-1} \mathcal{A}_{fl} v_l^*(t)$ is the target velocity of the followers based on the velocity of the leaders according to Lemma 5.

Consider the candidate Lyapunov function as follows:

$$V(t) = \frac{1}{2} \|\delta\|^2 = \frac{1}{2} \|q - q^*\|^2. \tag{46}$$

Take the time derivative of V, which can be represented as follows:

$$\begin{aligned}\dot{V}(t) &= (q-q^*)^T\bar{E}^T\mathrm{diag}\Big(P_{g_k}(D^c)^T\Big)\Big(\mathrm{sig}\big(\mathrm{diag}(D^cP_{g_k})g^c\big)^\tau \\ &\quad +\mathrm{sig}\big(\mathrm{diag}(D^cP_{g_k})g^c\big)^\rho\Big) \\ &= -(q^*)^T\bar{E}^T\mathrm{diag}\Big(P_{g_k}(D^c)^T\Big)\Big(\mathrm{sig}\big(\mathrm{diag}(D^cP_{g_k})g^c\big)^\tau \\ &\quad +\mathrm{sig}\big(\mathrm{diag}(D^cP_{g_k})g^c\big)^\rho\Big) \\ &= -(e^*)^T\mathrm{diag}\Big(P_{g_k}(D^c)^T\Big)\Big(\mathrm{sig}\big(\mathrm{diag}(D^cP_{g_k})g^c\big)^\tau \\ &\quad +\mathrm{sig}\big(\mathrm{diag}(D^cP_{g_k})g^c\big)^\rho\Big) \\ &= -\sum_{k=1}^{m}(e_k^*)^TP_{g_k}(D^c)^T\Big(\mathrm{sig}\big(D^cP_{g_k}g_k^c\big)^\tau+\mathrm{sig}\big(D^cP_{g_k}g_k^c\big)^\rho\Big) \\ &= -\sum_{k=1}^{m}\|e_k^*\|\sum_{i=1}^{d}\Big(\big|\big[D^cP_{g_k}g_k^c\big]_i\big|^{\tau+1}+\big|\big[D^cP_{g_k}g_k^c\big]_i\big|^{\rho+1}\Big) \\ &\le -\theta_d\sum_{k=1}^{m}\sum_{i=1}^{d}\left(\Big(\big|\big[D^cP_{g_k}g_k^c\big]_i\big|^2\Big)^{(\tau+1)/2}+\Big(\big|\big[D^cP_{g_k}g_k^c\big]_i\big|^2\Big)^{(\rho+1)/2}\right)\end{aligned}, \tag{47}$$

where $\theta_d=\min_{k=1,\ldots,m}\|e_k^*\|$, and apply Lemma 2 in the above inequality. Then, the following results can be obtained:

$$\begin{aligned}\dot{V} &\le -\theta_d\sum_{k=1}^{m}\left(\left(\sum_{i=1}^{d}\big|\big[D^cP_{g_k}g_k^c\big]_i\big|^2\right)^{(\tau+1)/2}+d^{(1-(\rho+1)/2)}\left(\sum_{i=1}^{d}\big|\big[D^cP_{g_k}g_k^c\big]_i\big|^2\right)^{(\rho+1)/2}\right) \\ &\le -\theta_d\sum_{k=1}^{m}\left(\Big(\big\|D^cP_{g_k}g_k^c\big\|^2\Big)^{(\tau+1)/2}+d^{(1-(\rho+1)/2)}\Big(\big\|D^cP_{g_k}g_k^c\big\|^2\Big)^{(\rho+1)/2}\right) \\ &\le -\theta_d\left(\left(\sum_{k=1}^{m}\big\|P_{g_k}g_k^c\big\|^2\right)^{(\tau+1)/2}+dm^{(1-(\rho+1)/2)}\left(\sum_{k=1}^{m}\big\|P_{g_k}g_k^c\big\|^2\right)^{(\rho+1)/2}\right) \\ &\le -\theta_d\left(\left(\sum_{k=1}^{m}g_k^TP_{g_k^c}g_k\right)^{(\tau+1)/2}+dm^{(1-(\rho+1)/2)}\left(\sum_{k=1}^{m}g_k^TP_{g_k^c}g_k\right)^{(\rho+1)/2}\right) \\ &\le -\theta_d\left(\left(\sum_{k=1}^{m}\frac{1}{\|e_k\|^2}e_k^TP_{g_k^c}e_k\right)^{(\tau+1)/2}+dm^{(1-(\rho+1)/2)}\left(\sum_{k=1}^{m}\frac{1}{\|e_k\|^2}e_k^TP_{g_k^c}e_k\right)^{(\rho+1)/2}\right)\end{aligned}. \tag{48}$$

The inequality can be further derived as follows by applying Lemma 3:

$$\begin{aligned}\dot{V} &\le -\frac{\theta_d}{\big(2s\sqrt{n-1}\big)^{\tau+1}}\left(\sum_{k=1}^{m}e_k^TP_{g_k^c}e_k\right)^{(\tau+1)/2}-\frac{\theta_d dm^{(1-(\rho+1)/2)}}{\big(2s\sqrt{n-1}\big)^{\rho+1}}\left(\sum_{k=1}^{m}e_k^TP_{g_k^c}e_k\right)^{(\rho+1)/2} \\ &\le -\xi_1\left(\sum_{k=1}^{m}e_k^TP_{g_k^c}e_k\right)^{(\tau+1)/2}-\xi_2\left(\sum_{k=1}^{m}e_k^TP_{g_k^c}e_k\right)^{(\rho+1)/2}\end{aligned}, \tag{49}$$

where $\xi_1=\theta_d\Big/\big(2s\sqrt{n-1}\big)^{\tau+1}$, $\xi_2=\Big(\theta_d dm^{(1-(\rho+1)/2)}\Big)\Big/\big(2s\sqrt{n-1}\big)^{\rho+1}$. Rewriting (44) as

$$\begin{aligned}\dot{V} &\le -\xi_1\left(\sum_{k=1}^{m}(e_k-e_k^*)^TP_{g_k^c}(e_k-e_k^*)\right)^{(\tau+1)/2}-\xi_2\left(\sum_{k=1}^{m}(e_k-e_k^*)^TP_{g_k^c}(e_k-e_k^*)\right)^{(\rho+1)/2} \\ &\le -\xi_1\Big(\delta^T\tilde{\mathcal{K}}^T(q^*)\tilde{\mathcal{K}}(q^*)\delta\Big)^{(\tau+1)/2}-\xi_2\Big(\delta^T\tilde{\mathcal{K}}^T(q^*)\tilde{\mathcal{K}}(q^*)\delta\Big)^{(\rho+1)/2}\end{aligned}. \tag{50}$$

Here, $\tilde{\mathcal{K}}(q^*) = \text{diag}\left(P_{g_k^c}\right)\bar{H}$. Under infinitesimal bearing rigidity of the target formation, the spectrum of $M^c = \tilde{\mathcal{K}}^\top \mathcal{K}$ contains precisely $d+1$ zero eigenvalues. We define $\theta_{d+2} \triangleq \min \sigma_{\neq 0}(M^c)$ as the minimal nonzero eigenvalue of M^c, where $\sigma_{\neq 0}$ denotes the nonzero spectrum. Since the deviation vector δ is orthogonal to the subspace $range(1_n \otimes I_d)$, and the null space of M^c satisfies $Null\left(\tilde{\mathcal{K}}^T\tilde{\mathcal{K}}\right) = Null\left(\tilde{\mathcal{K}}\right) = span\{range(1_n \otimes I_d), r^c\}$ as established in Lemma 4, the aforementioned inequality yields the following:

$$\begin{aligned} \dot{V} &\leq -\xi_1\left(\theta_{d+2}\|\delta\|^2 \sin^2\zeta\right)^{(\tau+1)/2} - \xi_2\left(\theta_{d+2}\|\delta\|^2\sin^2\zeta\right)^{(\rho+1)/2} \\ &\leq -\gamma_1 V^{(\tau+1)/2} - \gamma_2 V^{(\rho+1)/2} \end{aligned}, \tag{51}$$

where ζ is the angle between δ and $-r^c$, as shown in Figure 1, and $\gamma_1 = \xi_1\left(2\theta_{d+2}\sin^2\zeta\right)^{(\tau+1)/2}$, $\gamma_2 = \xi_2\left(2\theta_{d+2}\sin^2\zeta\right)^{(\rho+1)/2}$. δ approaches zero as time t progresses towards infinity, as illustrated in Figure 1. It follows from Lemma 1 that the convergence of V to zero occurs within a fixed time interval, estimated by $T_{\max} = (\pi\mu)/\left(2\sqrt{\gamma_1\gamma_2}\right)$.

Collision avoidance is a critical aspect of practical formation control problems, ensuring the safe and efficient operation of the agents within the system. It can be integrated with techniques such as artificial potential fields to ensure collision avoidance among agents. However, since that the only information available between agents is the relative bearing information, we establish a condition that guarantees collision avoidance throughout the formation maneuver. Assume that χ represents the specified minimum allowable separation between any pair of agents, which is required to fulfill the following condition:

$$0 \leq \chi < \min_{i,j\in\mathcal{V},t\geq 0}\left\|q_i^*(t) - q_j^*(t)\right\|. \tag{52}$$

For any $i, j \in \mathcal{V}$, the following equality always holds:

$$q_i(t) - q_j(t) \equiv \left[q_i^*(t) - q_j^*(t)\right] + \left[q_i(t) - q_i^*(t)\right] - \left[q_j(t) - q_j^*(t)\right]. \tag{53}$$

Therefore, the following can be obtained:

$$\begin{aligned} \left\|q_i(t) - q_j(t)\right\| &\geq \left\|q_i^*(t) - q_j^*(t)\right\| - \left\|q_i(t) - q_i^*(t)\right\| - \left\|q_j(t) - q_j^*(t)\right\| \\ &\geq \left\|q_i^*(t) - q_j^*(t)\right\| - \textstyle\sum_{k\in\mathcal{V}_f}\left\|q_k(t) - q_k^*(t)\right\| \\ &\geq \left\|q_i^*(t) - q_j^*(t)\right\| - \sqrt{n_f}\left\|q_f(t) - q_f^*(t)\right\| \\ &\geq \left\|q_i^*(t) - q_j^*(t)\right\| - \sqrt{n_f}\left\|\delta_q(t)\right\| \end{aligned}. \tag{54}$$

With the lower bound on $\left\|q_i(t) - q_j(t)\right\|$ known, the requirement that this bound remains greater than χ secures the minimum inter-agent distance. Consider the Lyapunov function (41), and the time derivative of V is $\dot{V} \leq -\gamma_1 V^{(\tau+1)/2} - \gamma_2 V^{(\rho+1)/2} \leq 0$. Consequently, it holds that $\left\|\delta_q(t)\right\| \leq \left\|\delta_q(0)\right\|$. By incorporating this inequality into Equation (43), the condition $\left\|q_i(t) - q_j(t)\right\| > \chi$ is satisfied provided that the initial value $\delta_q(0)$ meets the following requirement:

$$\left\|\delta_q(0)\right\| < \frac{\min_{i,j\in\mathcal{V},t\geq 0}\left\|q_i^*(t) - q_j^*(t)\right\| - \chi}{\sqrt{n_f}}. \tag{55}$$

Note that the condition above is considered conservative in practice because it is a sufficient condition.

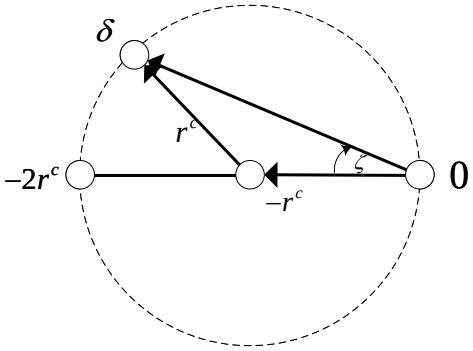


Figure 1. Illustration of the proof of fixed-time convergence.

4. Simulation

An eight-agent system in 3D space with bearing sensing topology $\mathcal{G}_b$ is deployed, as shown in Figure 2. The formation specification drives the swarm toward a cubic configuration, as visualized in Figure 2. To demonstrate the rapid convergence performance, we present a comparison between the proposed algorithm and an exponential convergence approach from the literature [40].

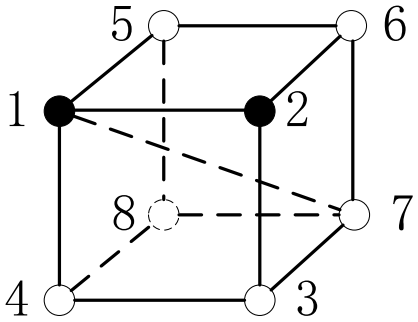


Figure 2. Bearing sensing topology $\mathcal{G}_b$.

Among the eight agents in Figure 2, agents 1–2 serve as velocity-invariant leaders in Figure 2, while the remaining six are followers. The desired set of bearing vectors is obtained based on the target configuration, where the positions of the agents are specified as follows: $q_1 = [0,0,0]^T$, $q_2 = [10,0,0]^T$, $q_3 = [10,0,-10]^T$, $q_4 = [0,0,-10]^T$, $q_5 = [0,-10,0]^T$, $q_6 = [10,-10,0]^T$, $q_7 = [10,-10,-10]^T$, and $q_8 = [0,-10,-10]^T$. The main parameters used in the orientation estimator and formation controller are shown in Table 1. The parameters listed in Table 1 are chosen in accordance with the fixed-time stability criteria established in Section 3. Specifically, a smaller $\alpha_1 \in (0,1)$ results in slower convergence in orientation estimation. The convergence time of formation control is jointly determined by parameters τ, ρ, κ_3, and κ_4. Parameters τ and ρ are determined by the value of μ, and a bigger $\mu > 1$ results in slower convergence in bearing-only formation control. Parameter κ_3 controls the descent rate of the Lyapunov function when the error is small, while parameter κ_4 governs the convergence slope when the error is large. Parameter κ_5 suppresses external disturbances; as long as $\kappa_5 > \bar{d}_i$, the convergence terms will dominate the disturbance, ensuring that $\dot{V} < 0$.

Table 1. Main parameters for orientation estimation and formation control.

α_1	τ	ρ	γ	κ_3	κ_4	κ_5
6/11	9/11	13/11	3/2	1	1	1

The following agents update their orientation estimates based on the fixed-time orientation estimation law (17). Figure 3 presents the simulation outcomes, where the estimated orientation is measured by the Frobenius norm $\left\|D_i\hat{D}_i^T - I_3\right\|_F$. It is evident that the estimator reaches a steady state corresponding to the common orientation D^c within a fixed time.

After the agents' orientations are successfully estimated, the formation control mechanism is subsequently engaged according to control law (34). The three-dimensional position errors for each agent are illustrated in Figure 4, while the root mean square error (RMSE) of these position deviations is presented in Figure 5. The individual bearing errors for each agent are illustrated in Figure 6, while the overall system bearing deviation, quantified by $\|g - g^*\|$, is presented in Figure 7. Red lines in Figures 5 and 7 denote the simulation results using a method that exponentially converges, as introduced in [40]. Agent trajectories in Figure 8 demonstrate predefined-time convergence to the target formation, achieving the desired configuration within rigorous time bounds.

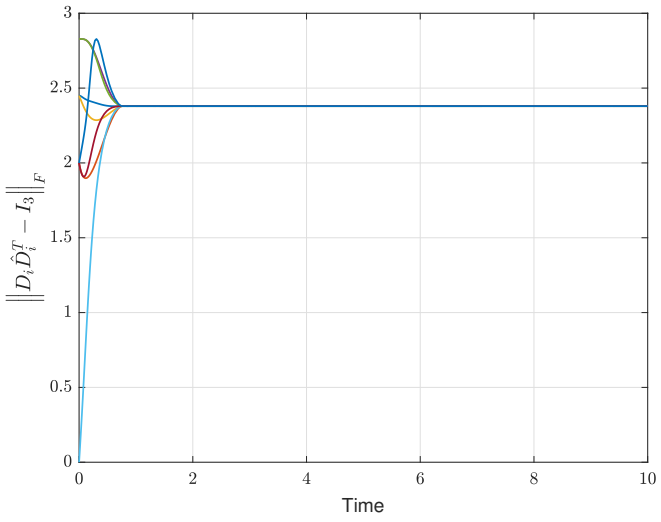


Figure 3. Fixed-time orientation estimation.

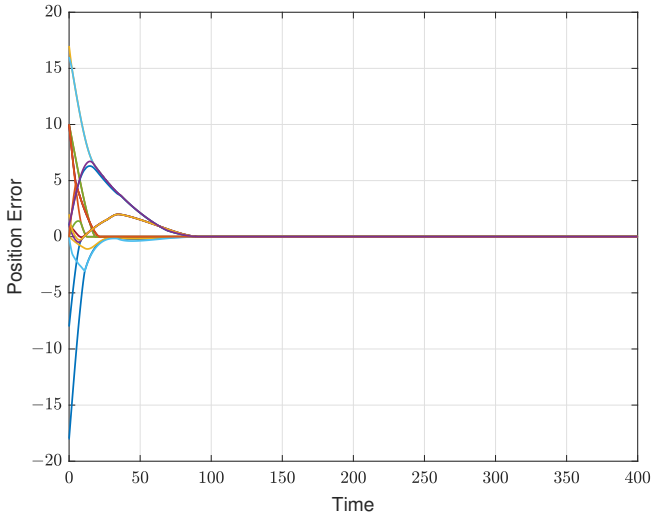


Figure 4. Position errors of formation control.

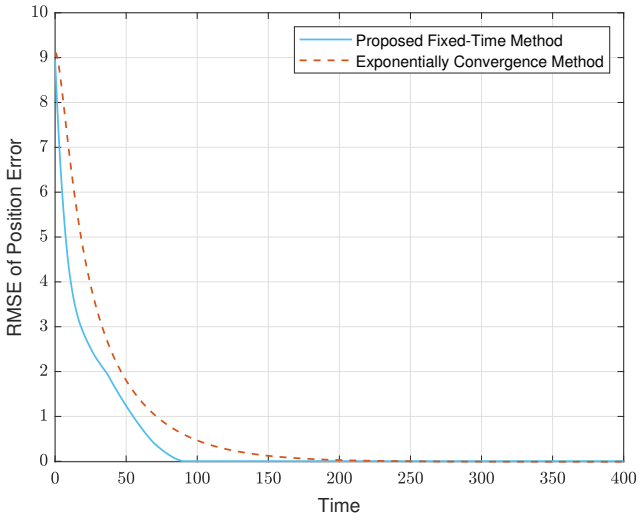


Figure 5. RMSE of position errors.

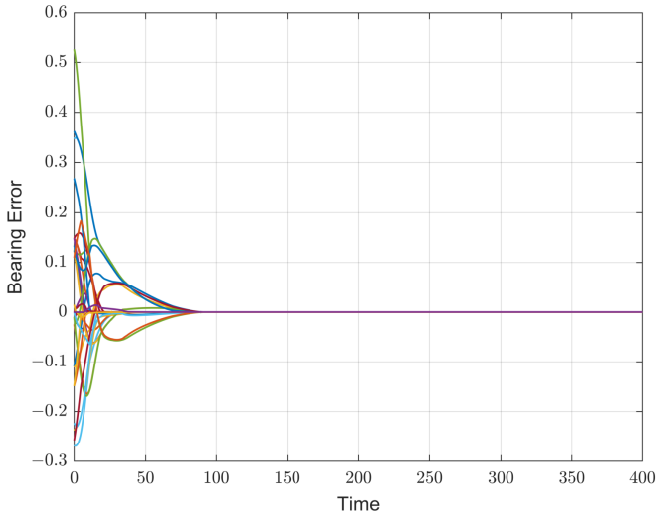


Figure 6. Bearing errors of formation control.

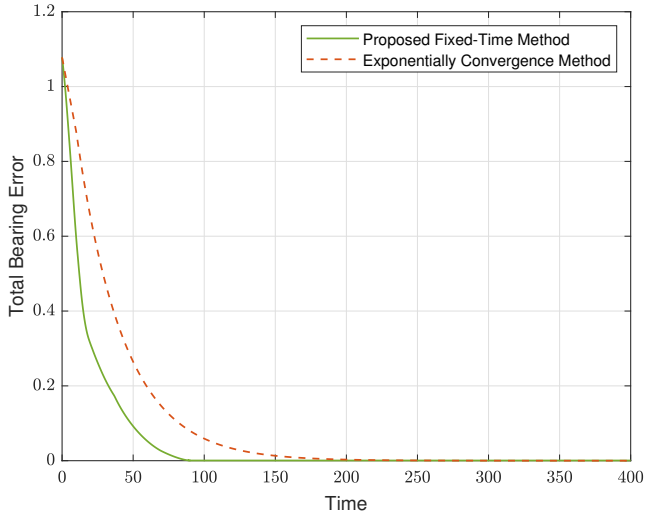


Figure 7. Bearing error of the entire system.

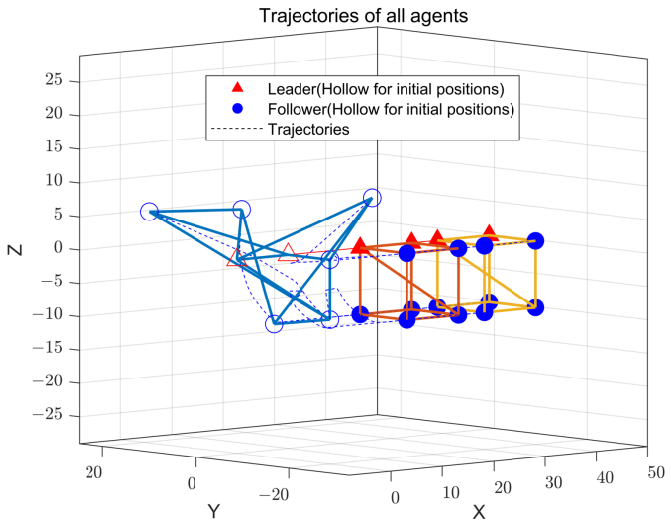


Figure 8. Trajectories of all agents.

5. Discussion and Conclusions

This study introduced an innovative formation control strategy using only bearing information, which was developed on top of a fixed-time orientation estimation approach. An orientation estimation scheme was devised, ensuring convergence within a guaranteed fixed time. Through comprehensive analysis of the convergence dynamics and near-global stability, it was demonstrated that the desired formation configuration was achievable from almost all initial conditions within a fixed time under the designed estimation and control framework.

The current study focused solely on undirected formations, and the development of fixed-time bearing-only control strategies for directed formations was left as a subject for future investigation. Additionally, bearing measurements are often affected by noise, which can propagate into the system dynamics. Investigating the impact of such noise is crucial for evaluating system performance. Meanwhile, the feasibility of executing orientation estimation law and formation control law simultaneously merits further investigation since the proposed control scheme requires both control laws to run separately. Finally, investigating fixed-time bearing-only formation strategies for agents governed by more complex dynamics constitutes a promising avenue for future study.

Author Contributions: Conceptualization, B.Z. and H.H.; methodology, B.Z., H.H., and M.L.; software, H.H. and M.L.; validation, M.L. and Q.W.; formal analysis, H.H. and M.L.; investigation, H.H.; resources, H.H. and M.L.; data curation, Q.W.; writing—original draft preparation, H.H. and M.L.; writing—review and editing, B.Z.; visualization, M.L. and Q.W.; supervision, B.Z.; project administration, B.Z. and H.H.; funding acquisition, B.Z. and H.H. All authors have read and agreed to the published version of the manuscript.

Funding: This research was supported by the National Natural Science Foundation of China (No. 62176214), the Guangdong Basic and Applied Basic Research Foundation (Grant No. 2023A1515011582), and the Fundamental Research Funds for the National Key Laboratory of Unmanned Aerial Vehicle Technology (No. WR202401).

Data Availability Statement: Most data are contained within the article.

Conflicts of Interest: The authors declare no conflicts of interest.

References

1. Yan, T.; Xu, Z.; Yang, S.X.; Gadsden, S.A. Formation control of multiple autonomous underwater vehicles: A review. *Intell. Robot.* **2023**, *3*, 1–22. [CrossRef]
2. Oh, K.K.; Park, M.C.; Ahn, H.S. A survey of multi-agent formation control. *Automatica* **2015**, *53*, 424–440. [CrossRef]
3. Oh, K.K.; Ahn, H.S. Distance-based undirected formations of single-integrator and double-integrator modeled agents in n-dimensional space. *Int. J. Robust Nonlinear Control* **2014**, *24*, 1809–1820. [CrossRef]
4. Sun, Z.; Mou, S.; Deghat, M.; Anderson, B.D. Finite time distributed distance-constrained shape stabilization and flocking control for d-dimensional undirected rigid formations. *Int. J. Robust Nonlinear Control* **2016**, *26*, 2824–2844. [CrossRef]
5. Smith, T.K.; Akagi, J.; Droge, G. Model predictive control for formation flying based on D'Amico relative orbital elements. *Astrodynamics* **2025**, *9*, 145–163. [CrossRef]
6. Zhou, H.; Jiao, B.; Dang, Z.; Yuan, J. Parametric formation control of multiple nanosatellites for cooperative observation of China Space Station. *Astrodynamics* **2024**, *8*, 77–95. [CrossRef]
7. Lei, B.; Shi, P.; Xu, Y.; Zhao, Y. Switching LPV control for electromagnetic formation flying on highly elliptical orbit. *Astrodynamics* **2021**, *5*, 373–389. [CrossRef]
8. Tron, R.; Thomas, J.; Loianno, G.; Daniilidis, K.; Kumar, V. A distributed optimization framework for localization and formation control: Applications to vision-based measurements. *IEEE Control Syst. Mag.* **2016**, *36*, 22–44.
9. Mao, G.; Fidan, B.; Anderson, B.D. Wireless sensor network localization techniques. *Comput. Netw.* **2007**, *51*, 2529–2553. [CrossRef]
10. Dong, Y.Y.; Dong, C.X.; Liu, W.; Chen, H.; Zhao, G.Q. 2-D DOA estimation for L-shaped array with array aperture and snapshots extension techniques. *IEEE Signal Process. Lett.* **2017**, *24*, 495–499. [CrossRef]
11. Midhun, E.; Ratnoo, A. Gap Traversal Guidance Using Bearing Information. *J. Guid. Control Dyn.* **2022**, *45*, 2360–2368. [CrossRef]
12. Nguyen, T.T.; Van Vu, D.; Van Pham, T.; Trinh, M.H. Bearing-Constrained Leader-Follower Formation of Single-Integrators with Disturbance Rejection: Adaptive Variable-Structure Approaches. *IEEE Trans. Cybern.* **2024**, *54*, 6283–6296. [CrossRef]
13. Wang, F.; Long, L. Switched-observer-based event-triggered adaptive fuzzy funnel control for switched nonlinear systems. *IEEE Trans. Fuzzy Syst.* **2021**, *30*, 1773–1787. [CrossRef]
14. Basiri, M.; Bishop, A.N.; Jensfelt, P. Distributed control of triangular formations with angle-only constraints. *Syst. Control Lett.* **2010**, *59*, 147–154. [CrossRef]
15. Bishop, A.N. Distributed bearing-only formation control with four agents and a weak control law. In Proceedings of the 2011 9th IEEE International Conference on Control and Automation (ICCA), Santiago, Chile, 19–21 December 2011; pp. 30–35.
16. Fabris, M.; Fattore, G.; Cenedese, A. Optimal time-invariant distributed formation tracking for second-order multi-agent systems. *Eur. J. Control* **2024**, *77*, 100985. [CrossRef]
17. Zhao, S.; Lin, F.; Peng, K.; Chen, B.M.; Lee, T.H. Finite-time stabilisation of cyclic formations using bearing-only measurements. *Int. J. Control* **2014**, *87*, 715–727. [CrossRef]
18. Li, Z.; Tnunay, H.; Zhao, S.; Meng, W.; Xie, S.Q.; Ding, Z. Bearing-only formation control with prespecified convergence time. *IEEE Trans. Cybern.* **2020**, *52*, 620–629. [CrossRef]
19. Erskine, J.; Briot, S.; Fantoni, I.; Chriette, A. Singularity Analysis of Rigid Directed Bearing Graphs for Quadrotor Formations. *IEEE Trans. Robot.* **2023**, *40*, 139–157. [CrossRef]
20. Zhao, S.; Li, Z.; Ding, Z. Bearing-only formation tracking control of multiagent systems. *IEEE Trans. Autom. Control* **2019**, *64*, 4541–4554. [CrossRef]
21. Zhao, S.; Zelazo, D. Localizability and distributed protocols for bearing-based network localization in arbitrary dimensions. *Automatica* **2016**, *69*, 334–341. [CrossRef]
22. Trinh, M.H.; Mukherjee, D.; Zelazo, D.; Ahn, H.S. Planar bearing-only cyclic pursuit for target capture. *IFAC-PapersOnLine* **2017**, *50*, 10136–10141. [CrossRef]
23. Trinh, M.H.; Oh, K.K.; Jeong, K.; Ahn, H.S. Bearing-only control of leader first follower formations. *IFAC-PapersOnLine* **2016**, *49*, 7–12. [CrossRef]
24. Trinh, M.H.; Mukherjee, D.; Zelazo, D.; Ahn, H.S. Formations on directed cycles with bearing-only measurements. *Int. J. Robust Nonlinear Control* **2018**, *28*, 1074–1096. [CrossRef]
25. Schiano, F.; Franchi, A.; Zelazo, D.; Giordano, P.R. A rigidity-based decentralized bearing formation controller for groups of quadrotor UAVs. In Proceedings of the 2016 IEEE/RSJ International Conference on Intelligent Robots and Systems (IROS), Daejeon, Republic of Korea, 9–14 October 2016; pp. 5099–5106.
26. Zhao, S.; Zelazo, D. Bearing rigidity and almost global bearing-only formation stabilization. *IEEE Trans. Autom. Control* **2015**, *61*, 1255–1268. [CrossRef]
27. Zhang, F.; Meng, D.; Zhang, J. Global Attitude Synchronization for Networked Rigid Bodies Under Directed Topologies. *IEEE Trans. Control Netw. Syst.* **2022**, *10*, 1362–1373. [CrossRef]

28. Wei, J.; Verginis, C.; Wu, J.; Dimarogonas, D.V.; Sandberg, H.; Johansson, K.H. Asymptotic and finite-time almost global attitude tracking: Representations free approach. In Proceedings of the 2018 European Control Conference (ECC), Limassol, Cyprus, 12–15 June 2018; pp. 3126–3131.
29. Mazare, M.; Asharioun, H.; Davoudi, E.; Mokhtari, M. Distributed finite-time neural network observer-based consensus tracking control of heterogeneous underwater vehicles. *Ocean Eng.* **2023**, *272*, 113882. [CrossRef]
30. Liang, X.; Zhang, Y.; Li, D.; Ge, S.S.; How, B.V.E.; Lee, T.H. Synchronized tracking control for dynamic positioning vessel. *Int. J. Robust Nonlinear Control* **2024**, *34*, 270–295. [CrossRef]
31. Lee, B.H.; Ahn, H.S. Distributed estimation for the unknown orientation of the local reference frames in n-dimensional space. In Proceedings of the 2016 14th International Conference on Control, Automation, Robotics and Vision (ICARCV), Phuket, Thailand, 13–15 November 2016; pp. 1–6.
32. Van Tran, Q.; Trinh, M.H.; Zelazo, D.; Mukherjee, D.; Ahn, H.S. Finite-time bearing-only formation control via distributed global orientation estimation. *IEEE Trans. Control Netw. Syst.* **2018**, *6*, 702–712. [CrossRef]
33. Li, H.; Zhu, M.; Chu, Z.; Du, H.; Wen, G.; Alotaibi, N.D. Fixed-time synchronization of a class of second-order nonlinear leader-following multi-agent systems. *Asian J. Control* **2018**, *20*, 39–48. [CrossRef]
34. Polyakov, A. Nonlinear feedback design for fixed-time stabilization of linear control systems. *IEEE Trans. Autom. Control* **2011**, *57*, 2106–2110. [CrossRef]
35. Zuo, Z.; Tie, L. A new class of finite-time nonlinear consensus protocols for multi-agent systems. *Int. J. Control* **2014**, *87*, 363–370. [CrossRef]
36. Li, J.; Fan, Y.; Liu, J. Distributed fixed-time formation tracking control for multiple underactuated USVs with lumped uncertainties and input saturation. *ISA Trans.* **2024**, *154*, 186–198. [CrossRef]
37. Bhat, S.P.; Bernstein, D.S. Finite-time stability of continuous autonomous systems. *SIAM J. Control Optim.* **2000**, *38*, 751–766. [CrossRef]
38. Parsegov, S.; Polyakov, A.; Shcherbakov, P. Fixed-time consensus algorithm for multi-agent systems with integrator dynamics. *IFAC Proc. Vol.* **2013**, *46*, 110–115. [CrossRef]
39. Mesbahi, M.; Egerstedt, M. *Graph Theoretic Methods in Multiagent Networks*; Princeton University Press: Princeton, NJ, USA, 2010; Volume 33.
40. Zhao, S.; Zelazo, D. Translational and scaling formation maneuver control via a bearing-based approach. *IEEE Trans. Control Netw. Syst.* **2015**, *4*, 429–438. [CrossRef]

Disclaimer/Publisher's Note: The statements, opinions and data contained in all publications are solely those of the individual author(s) and contributor(s) and not of MDPI and/or the editor(s). MDPI and/or the editor(s) disclaim responsibility for any injury to people or property resulting from any ideas, methods, instructions or products referred to in the content.